

Thermal–hydraulic study of the Primary Heat Transport System of the EU-DEMO Divertor Plasma Facing Components

S. Vacca^{a,*}, G. Agnello^a, G. Bongiovì^a, F.M. Castrovinci^a, P. Chiovaro^a, P.A. Di Maio^a,
F. Maviglia^b, I. Moscato^b, A. Quartararo^a, M. Siccino^{b,c}, E. Vallone^a

^a Department of Engineering, University of Palermo, Viale delle Scienze, Ed. 6, 90128 Palermo, Italy

^b EUROfusion Consortium, PPPT Department, Boltzmannstr. 2, Garching, Germany

^c Max Planck Institute of Plasma Physics (E2M), Boltzmannstr. 2, 85748 Garching, Germany

ARTICLE INFO

Keywords:

DEMO
Divertor
Plasma Facing Components
PHTS
Thermal hydraulics

ABSTRACT

A DEMONstration fusion reactor (EU-DEMO) is currently being developed by the EUROfusion consortium, in line with the Horizon Europe research framework programme. This fusion device will be the first on a large scale to generate net electricity. The EU-DEMO reactor is anticipated to undergo a pulsed duty cycle under normal operating conditions, which could shorten the qualified lifetime of the main equipment due to the inevitable induced mechanical and thermal cycling. Furthermore, the plasma control strategy envisaged for the EU-DEMO reactor foresees the potential occurrence of planned and unplanned plasma over-power transients, which might harm the plasma-facing components structure. In light of this, it is essential to dispose of reliable means to predict the thermal–hydraulic performance of the Primary Heat Transport Systems (PHTSs). Given this background, the University of Palermo, in partnership with the DEMO Central Team (DCT), has embarked on a research programme to evaluate the thermal–hydraulic response of the DIVertor Plasma-Facing Components (DIV PFC) PHTS under normal and upset conditions. To this purpose, in order to capture all the relevant geometric, hydraulic and thermal features associated with both ex-vessel and in-vessel components, a detailed finite-volume model has been developed. Next, the analysis of the thermal–hydraulic performance of the DIV PFC PHTS has been conducted both under hypothetical steady-state conditions and during the standard DEMO power cycle. The scope of the activity has been to verify whether the current design of the PHTS is capable of withstanding the pulsating loads it is expected to undergo under nominal conditions. The study has followed a theoretical–computational methodology founded on the use of the thermal–hydraulic system code TRACE. The hypotheses, models and results of the study are presented and commented.

1. Introduction

In order to harness nuclear fusion reactions for large-scale electrical power generation, the EUROfusion consortium is working on the design of a DEMONstration fusion reactor (EU-DEMO) [1], which is meant to be the next step after ITER in the quest to exploit fusion energy [2]. Since the EU-DEMO is anticipated to deliver net electricity to the grid, it is essential to correctly assess the relevant features of the energy conversion and cooling systems. These systems are an integral part of the realization and licencing process of the entire facility.

Since the Tokamak architecture is the basis of the EU-DEMO, it is expected to follow a pulsed duty cycle under normal operating conditions [3]. This aspect poses significant challenges for the design of the principal elements of the heat transport systems, as they may suffer a reduction in qualified lifetime due to the mechanical and thermal

cycling they may be subjected to during normal operations. Furthermore, the plasma control strategy envisaged for the EU-DEMO foresees the potential occurrence of planned and unplanned plasma over-power transients [4] that could damage the structural integrity of plasma-facing components. It follows that, from the earliest design stages, the identification of the correct control strategies for the Primary Heat Transport Systems (PHTSs) is crucial to keep key thermal–hydraulic parameters tightly controlled under all conditions the reactor may have to operate. In this context, it is essential to have reliable tools to predict the thermal–hydraulic performance of the PHTSs.

Given this background, the University of Palermo (UNIPA), in cooperation with the DEMO Central Team (DCT), has commenced a research campaign to investigate the thermal–hydraulic performance of the PHTS of the DIV PFCs under normal and upset conditions.

* Corresponding author.

E-mail address: silvia.vacca@unipa.it (S. Vacca).

<https://doi.org/10.1016/j.fusengdes.2024.114241>

Received 24 November 2023; Received in revised form 9 February 2024; Accepted 10 February 2024

Available online 13 February 2024

0920-3796/© 2024 The Authors. Published by Elsevier B.V. This is an open access article under the CC BY license (<http://creativecommons.org/licenses/by/4.0/>).

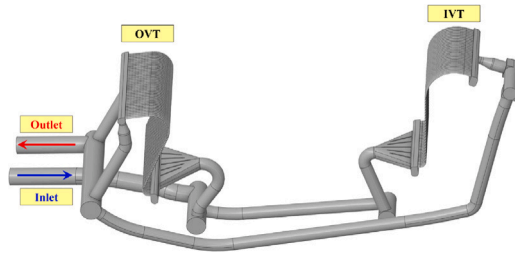


Fig. 1. The DEMO DIV PFCs.

To this end, a detailed finite-volume model has been developed with the aim of catching all the relevant geometric, hydraulic and thermal features of components inside and outside the vessel. Afterwards, attention has been concentrated on the analysis of the thermal–hydraulic performance of the DIV PFC PHTS under hypothetical steady-state conditions analogous to those relevant to the pulse phase of the EU-DEMO duty cycle in order to verify the distribution of the Mass Flow Rates (MFRs) among the DIV PFCs and the pressure drops along the entire circuit. In a second phase, efforts have been directed at studying the thermal–hydraulic performances of the DIV PFC PHTS under the transient conditions expected during normal operations and, in particular, a parametric study has been conducted in order to assess how the duration of the transition phases envisaged during the EU-DEMO duty cycle would affect the main thermal–hydraulic parameters that characterise the system.

The study has been performed in accordance with a theoretical–computational approach employing the TRACE thermal–hydraulic system code version 5.0 patch 7 [5].

The assumptions, models and results of the study are presented and critically commented.

2. The design of the DIV PFC PHTS

The divertor plays a fundamental role in a nuclear fusion reactor as it is responsible for power extraction and impurity removal via guided plasma exhaust [6]. The practicability of fusion power generation is closely related to thermal loads that the DIV PFCs is capable of withstanding under normal and off-normal operations [1]. Hence, its cooling system must be designed, from a thermal–hydraulic point of view, with a great care, to operate safely and reliably.

The DIV PFC assembly comprises an Inner Vertical Target (IVT) and an Outer Vertical Target (OVT) [7] which are connected in parallel by three-way branching to the inlet and outlet manifolds and are composed of a toroidal arrangement of, respectively, 31 and 43 Plasma Facing Units (PFUs) fed by properly shaped headers (see Fig. 1). The PFU design is based on the ITER tungsten monoblock concept [8], which consists of a cooling tube made of a CuCrZr alloy covered by thick tungsten tiles, these are coupled by a thin copper layer to accommodate their differential thermal expansion. The PFU cooling channels are equipped with copper twisted tapes to improve heat transfer efficiency. The DIV PFC PHTS serves as both a containment boundary for the primary coolant and a means of removing thermal power from the DIV PFCs and transferring it to the Power Conversion System (PCS). The DIV PFC PHTS operates with water at 5 MPa (DIV PFCs inlet pressure) and 130/136 °C [9]. Preliminary equipment sizing is conducted considering a reference thermal power of 142 MW.

The latest version of the DIV PFC PHTS consists of a single cooling system that feeds all the DIV PFC cooling circuits in parallel (see Fig. 2).

The system is composed of two subsections arranged in series, each feeding the DIV PFCs belonging to half a tokamak, and is connected to a pressurizer that performs the pressure control function. A single

Table 1

DIV PFC PHTS design data.

Total thermal power [MW]	142
Total pumping power [MW]	19
DIV PFC inlet/outlet temperature [°C]	130/136
Loop MFR [kg/s]	2779
Total water volume [m ³]	189
Total piping length [m]	2854
Cooling loops [-]	1

subsection comprises a pump, a cold leg, a cold ring header, 24 cold feeding manifolds, 24 hot feeding manifolds, a hot ring header, a hot leg, a heat exchanger and a cross-over pipe. The relevant design data of the DIV PFC PHTS [10] are shown in Table 1.

3. The thermal–hydraulic analysis campaign

In light of the activities promoted by the EUROfusion consortium, UNIPA, in collaboration with the DCT, have commenced a research campaign to study the thermal–hydraulic performance of the DIV PFC PHTS under normal and upset conditions.

Therefore, a detailed finite volume model has been developed with the aim of capturing all the main geometric, hydraulic and heat transfer features of both ex-vessel and in-vessel components. Thereafter, attention has been focused on the analysis of the thermal–hydraulic performance of the DIV PFC PHTS under hypothetical steady-state conditions analogous to those that would occur during the pulse phase of the EU-DEMO duty cycle, in order to verify the distribution of MFRs among the DIV PFCs and the pressure drops along the entire circuit. Besides, a comparison with analytical data has been conducted to verify the efficaciousness of the constructed model in forecasting the performance of the DIV PFC PHTS. In a second phase, efforts have been turned to the study of the thermal–hydraulic performances of the DIV PFC PHTS under the transient conditions expected during normal operation. Specifically, a parametric study has been conducted to evaluate how the duration of the transition phases foreseen during the EU-DEMO duty cycle affects the main thermal–hydraulic parameters that characterise the system.

A theoretical–computational approach has been adopted for the present research work and the TRACE thermal–hydraulic system code version 5.0 patch 7 has been used.

3.1. Investigated scenarios

The heat loads adopted in this activity are based on the normal operation, steady-state baseline EU-DEMO plasma scenario (see [11]). The total power of the Scrape-Off Layer (SOL) has been increased, conservatively channelling this increased power to the particles impacting the divertor targets. In particular, it is expected that the DEMO nuclear fusion reactor will be able to operate in a range of plasma operating regimes, which means that the power deposited on an individual component can vary within certain limits between one operating regime and another. Therefore, in order to establish a challenging but realistic operating scenario for the divertor, it was decided to increase the power deposited in the SOL by 20%. In fact, a larger increase in deposited power would have been unrealistic, while a smaller increase would have been less indicative of divertor operation. Under these assumptions, the power breakdown depicted on the left side of Fig. 3 is obtained.

Considering the selected EU-DEMO plasma scenario, the heat loads over the divertor targets can be realistically estimated starting from the outcomes of neutronics [12] and plasma-physics [13,14] simulations. As reported in the right part of Fig. 3, the total power obtained is ≈ 126 MW, which is close to but lower than the DIV PFC PHTS design value of 142 MW. In this regard, it is worth highlighting that the design

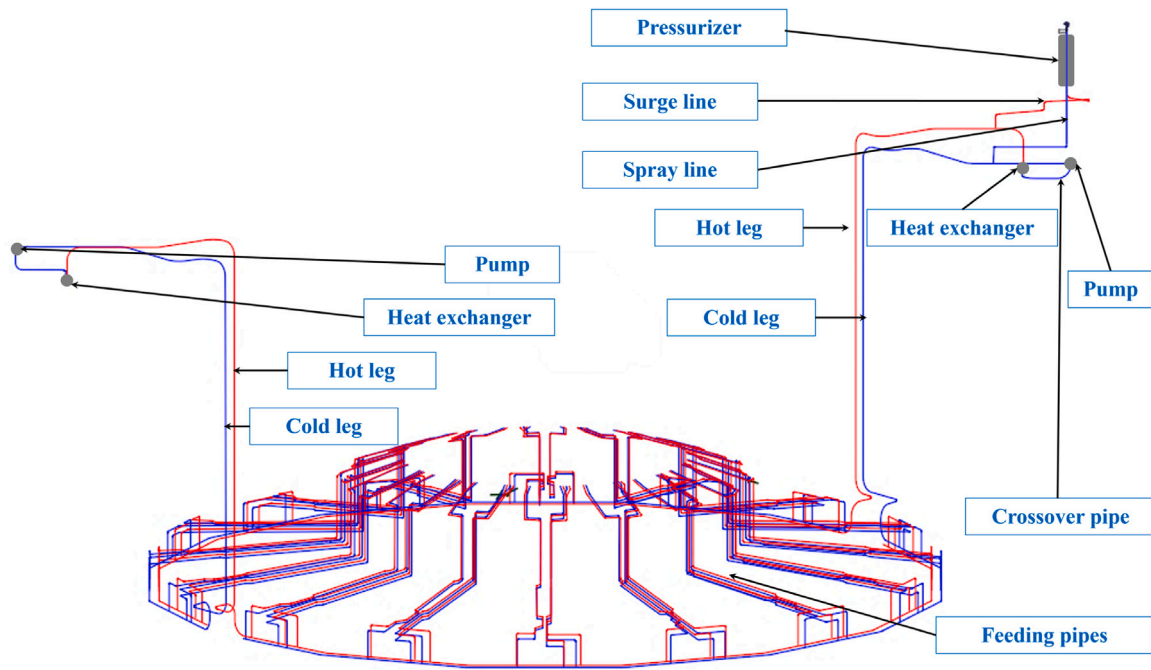


Fig. 2. Layout of the DIV PFC PHTS.

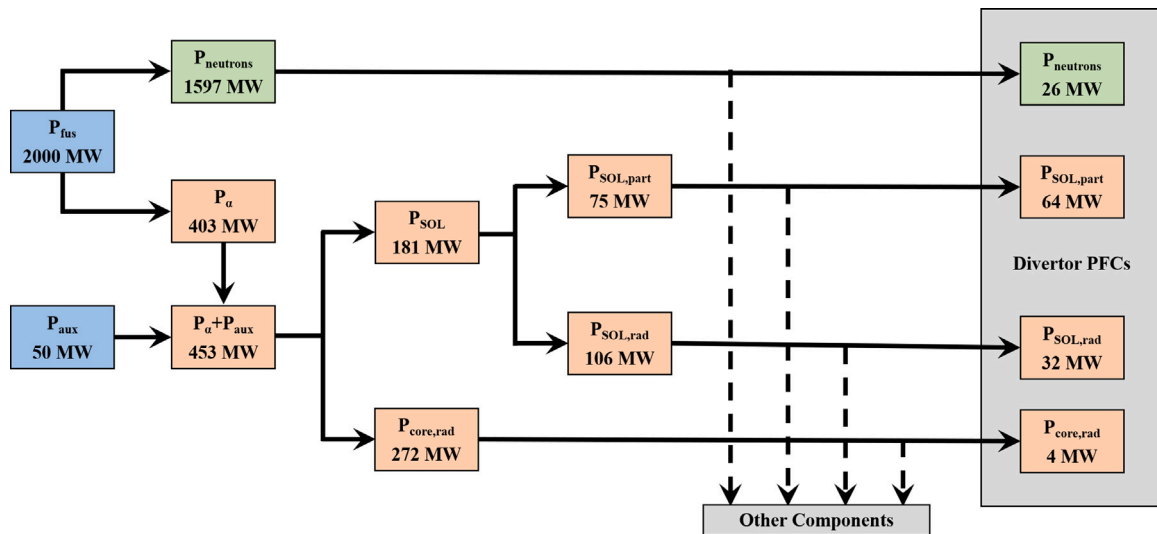


Fig. 3. Assumed breakdown of the heating power originating from the EU-DEMO plasma.

value of power take into account margins for the thermal sizing of the equipment.

Concerning the non-neutronic loads, other observations are needed to fully determine how the power values and the power profile distributions have been determined. As described in [15], separate analyses are required to obtain the different contributions of power carried by core and SOL electromagnetic radiation, charged particles, and neutrals. In the EU-DEMO group, the kinetic profiles for the core region are usually estimated with the 1.5D code ASTRA [16], then they are used as input into the Monte-Carlo ray-tracing code CHERAB [17] to evaluate the core radiative heat loads on the divertor structures. The remaining heat flux contributions are estimated by employing the edge plasma solver SOLPS [18] in the limit of fluid neutrals. The flat-top results of ASTRA-CHERAB [13] and those of SOLPS [14] are used here to evaluate the heat fluxes during the pulse phase, obtained under the assumption of the divertor operated in detached mode. These profiles have been

properly scaled to have a set of data consistent with the plasma power breakdown of Fig. 3. It must be emphasized that the present SOLPS calculation does not consider the 3D structures that are located in the first wall, e.g. limiters, which may intercept a small part of the load carried by charged particles in the external regions of the SOL, otherwise directed to the divertor. This additional contribution to the divertor power is conservatively neglected [15]. Taking into account that different divertor geometries have been investigated in ASTRA-CHERAB and SOLPS calculations, as visible in Fig. 4, two additional pre-processing steps have been required for the heat flux data. In particular, the geometry of the SOLPS simulation has been adjusted by a proper uniform scaling of the OVT corner, saving the total power deposited on the component. Afterwards, the core radiation term has been interpolated over the SOLPS rescaled computational domain, so to have a single distribution of heat flux, comprehensive of the four contributions previously reported, to be used in TRACE calculation.

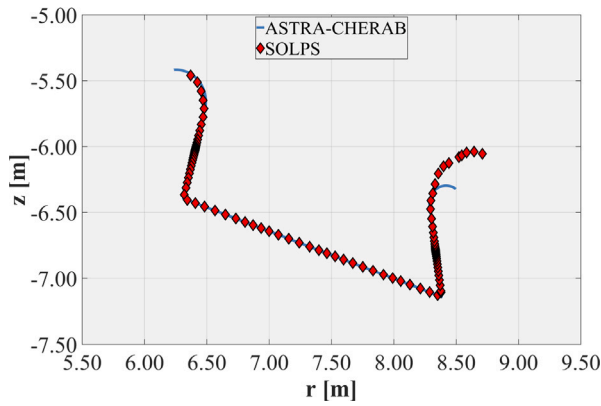


Fig. 4. Computational domains used in plasma-physics calculations.

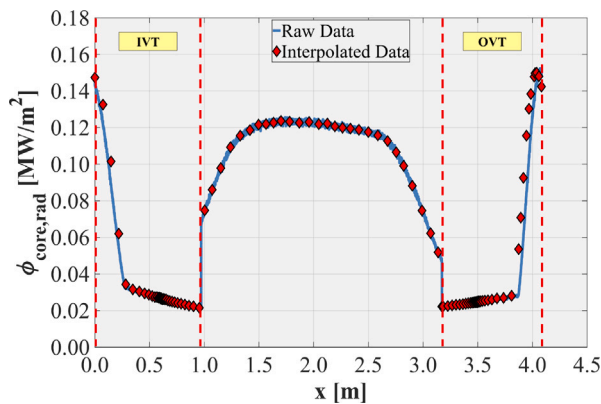


Fig. 5. Interpolated results obtained.

Table 2
Integral power breakdown for the DIV PFC.

	OVT	IVT	Total
Core Radiation [MW]	2	2	4
SOL Radiation [MW]	16	16	32
Particles [MW]	41	23	64
Neutrons [MW]	14	12	26
Total [MW]	73	53	126

Starting from the j th node (r_j, z_j) of the ASTRA-CHERAB model, the interpolated result on the i th SOLPS node (r_i, z_i) has been obtained according to Eq. (1), where N is the number of nodes of the ASTRA-CHERAB spatial discretization and $w_{i,j}$ is a weight function. This latter is calculated according to Eq. (2), where $\|d_{i,j}\|$ is the distance between nodes i and j while α and d_{max} are the interpolator free parameters.

$$\phi_{core,rad}(r_i, z_i) = \sum_{j=1}^N w_{i,j} \phi_{core,rad}(r_j, z_j) \quad (1)$$

$$w_{i,j} = \begin{cases} \frac{e^{-\left(\alpha \frac{\|d_{i,j}\|}{d_{max}}\right)^2}}{\sum_{k=1}^N w_{i,k}} & \text{if } \|d_{i,j}\| \leq d_{max} \\ 0 & \text{otherwise} \end{cases} \quad (2)$$

Fig. 5 shows the raw and interpolated data along the divertor profile. The total heat flux deposition profile estimated for a detached divertor in steady-state conditions is reported in Fig. 6, while the heat flux breakdown is in Fig. 7. Then, integrating the heat flux profiles over the pertaining surfaces and considering the nuclear heating, the overall power deposited on the 48 DIV PFCs can be calculated, as reported in Table 2.

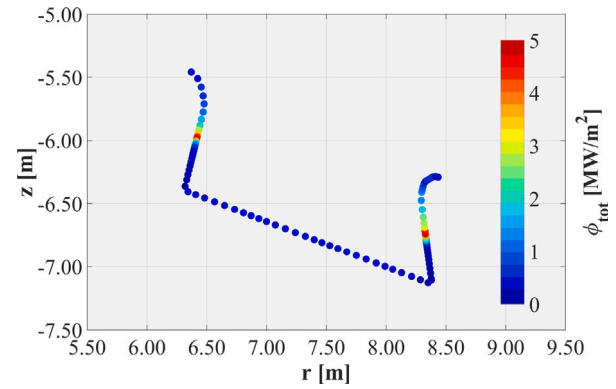


Fig. 6. Total heat flux deposition profile in steady-state condition.

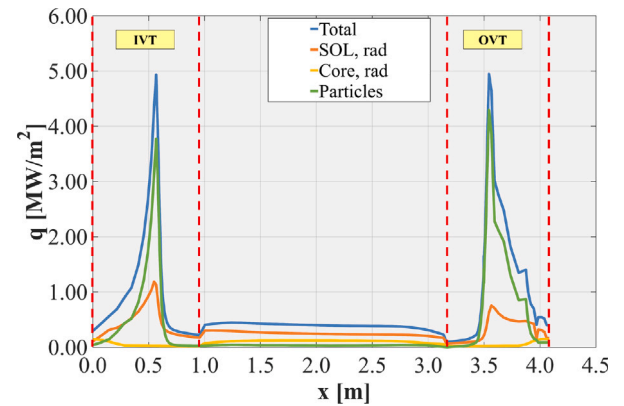


Fig. 7. Heat flux breakdown in the different regions of the divertor.

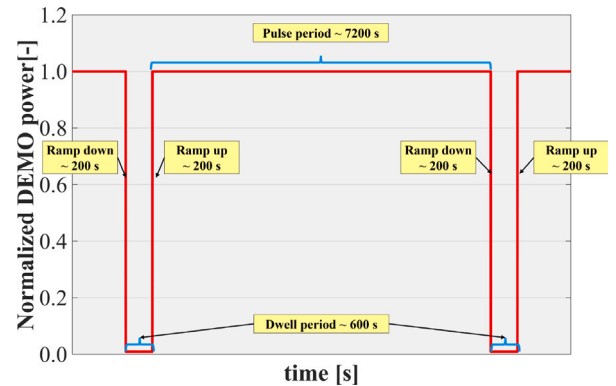


Fig. 8. EU-DEMO duty cycle.

The thermal loads described above vary over time according to the EU-DEMO duty cycle (see Fig. 8).

The reference duty cycle includes two main periods in which the reactor power varies from 100% to a minimum of about 1/2% of its nominal value, predominantly because of the residual heat in the tokamak structures. The two periods, referred to as pulse and dwell, endure for roughly 2 h and about 10 min respectively. The passage from pulse period to dwell and vice versa takes place through two transition phases, known as the plasma ramp-down and ramp-up. The reference ramps last approximately 200 s each.

However, recent design needs have highlighted that these transition phases could last longer, approximating and even exceeding 600 s. Therefore, as already mentioned, it has been deemed necessary to carry out a parametric study on the duration of the ramps in order to assess

Table 3

Transient scenarios.

Case	Pulse [s]	Ramp down [s]	Dwell [s]	Ramp up [s]
1	7200	100	600	100
2	7200	200	600	200
3	7200	400	600	400
4	7200	600	600	600
5	7200	1000	600	1000

their effect on the principal components of the DIV PFC PHTS and, specifically, the cases depicted in Table 3 have been examined.

In this respect, it is worth emphasising that, for the purposes of this calculation, it has been assumed that the thermal loads vary linearly during the transition phases (i.e. ramp up and ramp down). Although reasonable, this assumption is not conservative given the inevitable power spikes to which the divertor is subjected during the transitions. In particular, the heat flux on the plasma-facing surface and the nuclear power deposited inside the PFUs coolant, have been assumed to vary from their nominal value during the pulse phase to zero during the dwell period. As for the nuclear power stored in the structure of the PFUs, it has been made to vary from its nominal value during the pulse phase to a value which corresponds to the residual decay heat at shutdown during the dwell period [19].

4. Model setup

Since the DIV PFC PHTS consists of a single cooling circuit, attention has been focused from the beginning on the modelling of the entire system. In particular, in line with the requirements of the TRACE system code, emphasis has been placed on the development of an accurate finite-volume model able to capture all the relevant thermal-hydraulic features characterising components inside and outside the vessel. Actually, the computational model comprises of four main sub-models:

- the geometrical sub-model, which replicates the layout of the PHTS in a quasi-2D approximation;
- the constitutive sub-model, which is supplied to the code for the description of the thermodynamic behaviour of the water flowing within the cooling system;
- the hydraulic sub-model, which is intended to simulate the fluid flow across the PHTS;
- the thermal sub-model, composed of several sub-models that are intended to realistically simulate the heat transfer phenomena in the cooling system.

The following sections of the paragraph describe each of the above-mentioned TRACE sub-models in detail.

4.1. Geometrical sub-model

In order to study the thermal-hydraulic performance of the DIV PFC PHTS under normal and off-normal conditions, a quasi-2D geometric model has been developed that effectively reproduces the flow domain of its circuit.

The discretization of the flow domain has been done while preserving the volume of each component, allowing for an accurate modelling of the total amount of coolant. In addition, subvolumes have been correctly placed to mimic their relative locations and heights. In this way, both gravitational effects and distributed pressure losses have been modelled meticulously, at least in terms of the geometric parameters that are used to evaluate them. Moreover, the nodalisation of the model has been developed so that reliable and realistic predictions of the thermal-hydraulic performance of the entire circuit can be obtained, while still requiring reasonable calculation times.

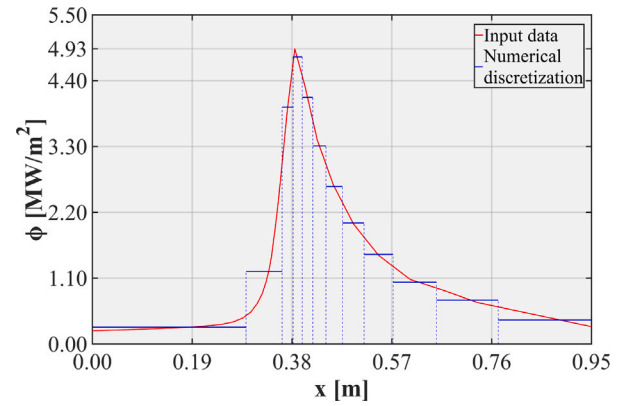


Fig. 9. Ducting discretization and heat flux profile of the IVT.

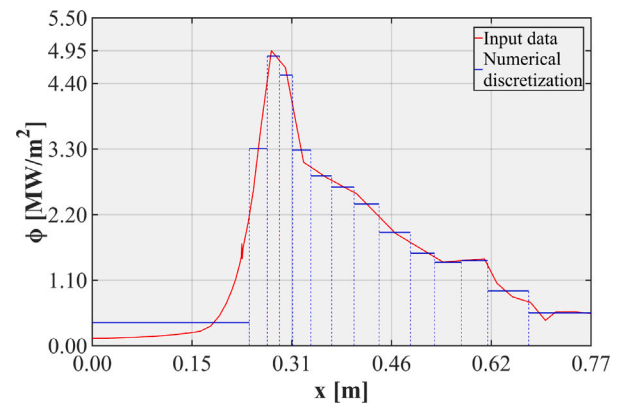


Fig. 10. Ducting discretization and heat flux profile of the OVT.

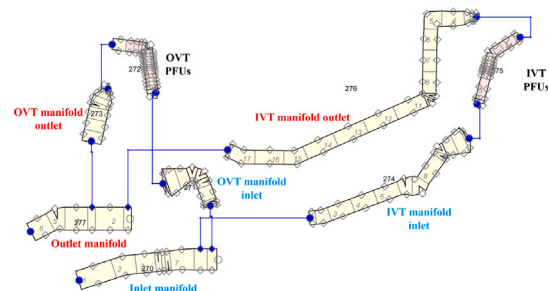


Fig. 11. TRACE model of the DIV PFC.

In this respect, an algorithm has been developed in a MATLAB [20] environment to optimise the discretization of the PFU channels in order to capture the heat flux distribution previously derived from the plasma physics calculations (see Fig. 7) while ensuring reasonable calculation times. In particular, the optimisation algorithm developed allows the overall power deposited on the PFU channels to be preserved, as well as the peak heat flux at the strike points, in order to correctly predict any thermal crisis phenomena that may occur within the PFU channels. Figs. 9 and 10 show a comparison between the previously derived heat flux curve and the discretized trend implemented in the TRACE model for IVT and OVT respectively.

Figs. 11 and 12 show a portion of the model developed on TRACE, in which the DIV PFCs and of the heat exchangers are represented respectively.

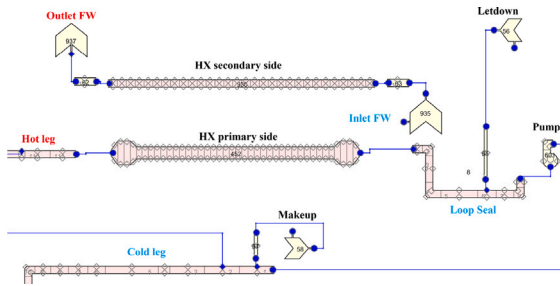


Fig. 12. TRACE model of the heat exchangers.

4.2. Constitutive sub-model

The behaviour of the water coolant circulating within the DIV PFC PHTS has been described using the constitutive models provided by the TRACE system code, for which the thermophysical properties of the coolant are given in special libraries as a function of pressure and temperature. Structural materials, when not available in the code, have been introduced by providing the thermophysical properties of each material in the form of tabular functions describing their functional dependence on temperature.

4.3. Hydraulic sub-model

The hydraulic model has been configured to adequately simulate the single-phase and/or two-phase water flow within the investigated cooling circuit. The concentrated and distributed hydraulic resistances have been modelled considering their possible functional dependence on the flow velocity field. In particular, the concentrated hydraulic resistances have been modelled through the well-known equation $\Delta p = K \rho \frac{v^2}{2}$, which relates the total pressure drop (Δp) to the flow velocity (v) via the concentrated loss factor (K), the values of which have been derived differently depending on whether one considers the in-vessel part, i.e. the DIV PFCs, or the ex-vessel part of the cooling circuit.

In order to catch the effect of the complex 3D structures of the DIV PFCs on their overall hydraulic behaviour, a specific modelling strategy has been used [21] that integrates the TRACE system code with the ANSYS CFX 3D Computational Fluid Dynamics (CFD) code [22]. Specifically, a detailed parametric analysis has been executed on the cooling circuit of the DIV PFCs [9] with the aim of evaluating the hydraulic characteristic functions of its main sections that give the functional dependence of their total pressure drop on the corresponding MFR (G) under steady-state conditions, i.e. $\Delta p = \alpha G^\beta$. More information about the procedure and the calculation models employed can be found in [9]. Subsequently, to properly reproduce the hydraulic behaviour of the DIV PFCs, this function has been used to obtain the dependence on Reynolds number (Re) of the concentrated effective hydraulic loss coefficients in the form $K = B Re^{-C}$ to be given as input to the TRACE system code.

On the other hand, as far as the ex-vessel PHTS is concerned, the relevant concentrated hydraulic loss coefficients have been derived from Idelchik handbook [23], which considers several geometric configurations and flow conditions. In this case, it is worth noting that since the concentrated hydraulic resistances are dependent on the spatial distribution of the flow velocity field, it has been assumed that the coolant flow distribution was that under normal operating conditions within the DIV PFC PHTS.

As far as the pump component is concerned, since a complete layout of the primary coolant pump of the DIV PFC PHTS is not yet available, the built-in Westinghouse characteristic curves have been preliminarily adopted [5].

Finally, the hydraulic wall roughness has been assumed according to [9,24] for the ex-vessel and in-vessel sections, respectively.

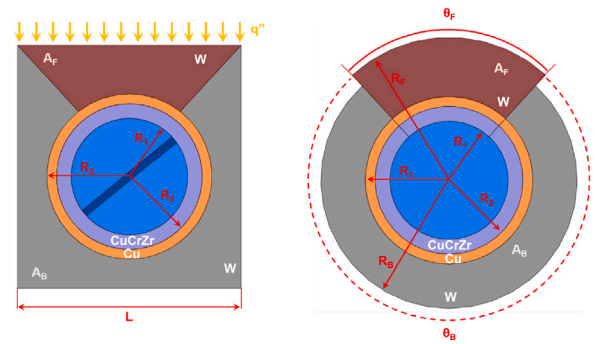


Fig. 13. The quasi-2D heat structure model of the tungsten monoblock.

4.4. Thermal sub-model

The model of the solid structures has been tailored to reproduce the actual thermal capacity of the system while preserving the heat fluxes to the coolant.

A special attention has been devoted to correctly simulate the complex 3D thermal-hydraulic behaviour of the PFU channels using the quasi-2D approach of the TRACE code, to reproduce the heat transfer characteristics of the real ITER-like PFU assembly [8]. It is indeed worth noting that only one face of the tungsten monoblock is heated directly by the plasma exhaust and, as highlighted by preliminary 3D CFD calculations, the heat flux distribution is mainly concentrated in the brown region highlighted on the left side of Fig. 13.

Since the TRACE system code only allows for cylindrical, spherical or slab type heat structures, it has been deemed necessary to develop a specific modelling approach to mimic the thermal behaviour of the tungsten monoblock. In order to correctly replicate the heat fluxes towards the coolant, the heat structure of the PFU channel has been arranged into two cylindrical annulus sectors (right side of Fig. 13), simulating the plasma-facing segment and the remaining part of the solid domain separately. The twisted tape has not been implemented, due to its negligible thermal inertia.

The main geometrical parameters of a typical PFU assembly shown in the left-hand side of Fig. 13 can be retrieved from [7]. On the other hand, the equivalent radius of the tungsten armour for the plasma-facing segment (R_F) and the remaining part of the solid domain (R_B), as well as their angular extent, θ_F and θ_B , respectively, have been obtained by solving the following system of equations, which permits reproducing the actual heat flux towards the coolant while saving the plasma-facing surface and the volume of the solid domain. A_F and A_B are the cross-section areas of the plasma-facing segment of the tungsten armour and the backside, respectively.

$$\begin{cases} R_F \theta_F = L \\ \frac{\theta_F}{2} (R_F^2 - R_3^2) = A_F \\ \theta_B = 2\pi - \theta_F \\ \frac{\theta_B}{2} (R_B^2 - R_3^2) = A_B \end{cases} \quad (3)$$

Regarding the Heat Transfer Coefficient (HTC) within the straight section of the plasma-facing channel where it is supposed to be located the swirl tape to enhance the coolant heat transfer capabilities, the TRACE system code does not envisage the presence of specific models for swirl tubes and adopts the default Gnielinski correlation [25] which perfectly applies to the straight tube case. Therefore, in order to predict with a reasonable accuracy the heat transfer at the fluid-wall interface within the plasma-facing swirl tube, an effective heat transfer diameter has been given in input to the code. Fig. 14 shows the HTC provided in the code compared to the one calculated with the correlation proposed by Manglik and Bergles in [26].

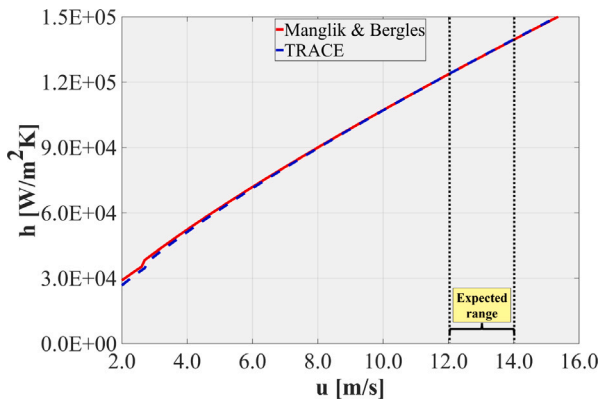


Fig. 14. TRACE modified HTC correlation.

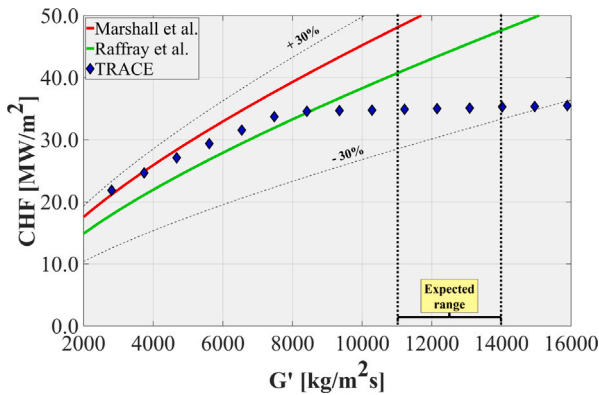


Fig. 15. TRACE modified CHF prediction.

A similar approach has been adopted for the Critical Heat Flux (CHF) calculation. The CHF is calculated by the TRACE system codes from the AECL CHF look-up table [27] because of its reasonably good accuracy and wide range of applicability. Therefore, in order to correctly predict the CHF within the swirl tubes, a CHF multiplier of ≈ 1.7 has been introduced. Fig. 15 shows a comparison of the CHF predicted by the code and the one calculated with the correlations reported in [28,29].

The CHF predicted by the code (see Fig. 15) follows the trend given by the correlations proposed by Marshall et al. [28] and by Raffray et al. [29] at low coolant mass fluxes while it is quite constant at the higher ones because the AECL CHF look-up tables adopted by the code do not extrapolate above their specific mass flux upper boundary (i.e. 8000 kg/m² s) corresponding to a coolant velocity of ≈ 9 m/s. Nevertheless, in the velocity range of interest expected during normal operation, the deviation of the predicted CHF from the one calculated with the correlation proposed by Raffray et al. [29] ranges between 15% and 25%. Moreover, at least in the velocity range of interest, the predicted CHF is always below the one calculated with the correlation which results in a conservative approach.

With regard to the thermal model developed for the ex-vessel part of the PHTS, the same procedure has been applied, with due distinctions, as in [24,30].

5. Preliminary steady-state analyses

As already mentioned, the study has been primarily concentrated on the evaluation of the thermal-hydraulic performance of the DIV PFC PHTS under hypothetical steady-state conditions that are similar to what would be encountered in the pulse phase of the EU-DEMO duty cycle. This part of the activity has provided the opportunity to check

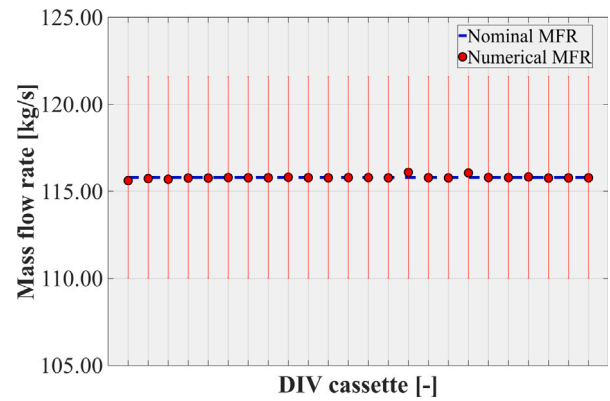


Fig. 16. MFR distribution among DIV PFC.

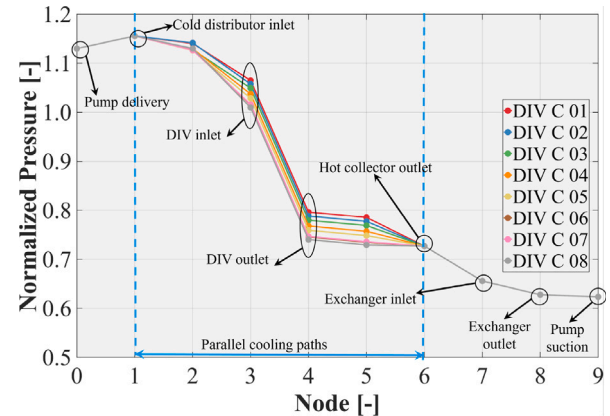


Fig. 17. Normalized pressure distribution in Central DIV PFC.

Table 4
Steady-state conditions.

	Analytical	Numerical	ϵ [%]
P_{Loop} [MW]	145	145	0.00
G_{Loop} [kg/s]	2779	2774	-0.17
ΔP_{Loop} [MPa]	2.50	2.54	1.64
$T_{Cold\ leg}$ [°C]	130.15	130.45	0.23
$T_{Hot\ leg}$ [°C]	135.87	135.55	-0.24
P_{PRZ} [MPa]	3.25	3.25	0.00
h_{PRZ} [m]	6.17	6.17	0.00
$P_{FW\ inlet}$ [MPa]	1.05	1.05	0.00
G_{FW} [kg/s]	187	180	-3.95
$T_{FW\ inlet}$ [°C]	39.10	39.10	0.00
$T_{FW\ outlet}$ [°C]	131.00	134.18	2.43

the distribution of MFRs among the DIV PFCs and the pressure drops along the entire circuit. Furthermore, it has been possible to make a comparison with available analytical data to prove the accuracy with which the model developed forecasts the behaviour of the DIV PFC PHTS. In this regard, the Table 4 shows a comparison between the analytical calculations and the numerical results. Furthermore, Fig. 16 shows the distribution of the MFR among the 24 cassettes placed in the half-loop of the DIV PFC PHTS, which are representative of all 48 cooling paths, compared with the nominal MFR with 5 % error bars. The pressure distribution throughout the cooling paths of the 8 central DIV PFCs is instead represented in Fig. 17.

From the outcomes obtained, it is possible to see the fundamental thermal-hydraulic parameters determined by the TRACE code closely match the values calculated analytically, as shown in Table 4. The maximum deviation is associated with the Feed Water (FW) MFR and amounts to approximately 4% of its nominal value. As far as the MFR

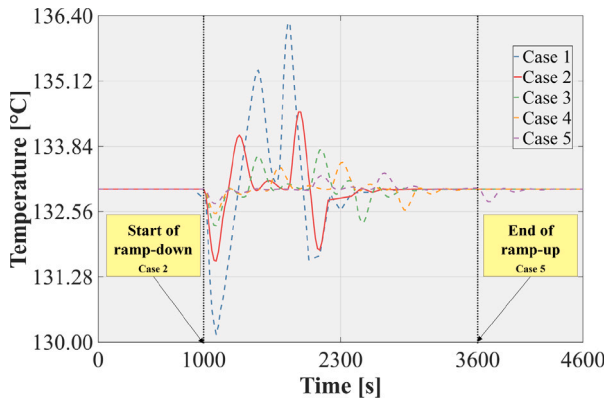


Fig. 18. Average temperature.

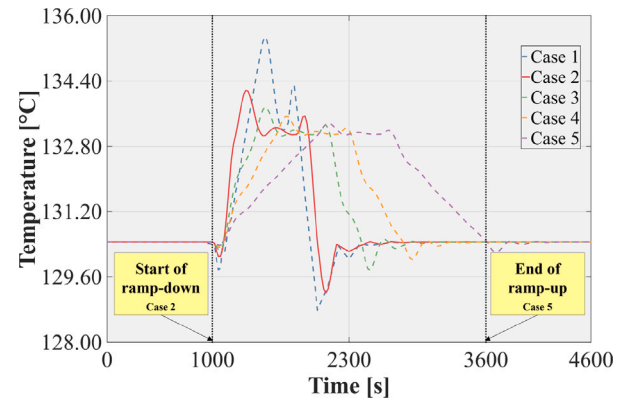


Fig. 19. Cold leg temperature.

distribution among the DIV PFCs is concerned, a uniform cooling distribution has been predicted, with a maximum deviation of about 0.3%. Finally, the predicted pressure distribution reproduces the analytical trend with a deviation of about 1.6% on the overall pressure drop, which amounts to about 2.54 MPa.

6. Transient analyses

In the second part of the analysis campaign, efforts have been directed at studying the thermal–hydraulic performances of the DIV PFC PHTS under the transient conditions expected during normal operation. As already explained in Section 3.1, a parametric study has been conducted on the ramp duration to evaluate its effect on the fundamental thermal–hydraulic parameters that characterise the system and, specifically, the cases reported in Table 3 have been examined. The calculations have included three entire pulse phases with associated dwell and transition periods (i.e. ramp-up and ramp-down) to verify that the system is capable of recovering the pulse steady-state conditions, but the main focus has been on the variation of the relevant thermal–hydraulic variables during the transition from pulse to dwell. The principal control systems have been set up building on the observations presented in [30].

The main results obtained for each of the scenarios investigated are given below. In particular, Figs. 18–20 show the average primary coolant temperature, the cold and hot leg temperature, respectively, while Fig. 21 illustrates the trend of the FW MFR on the secondary side of one of the two exchangers as it is representative of both. Finally, Figs. 22 and 23 show the pressurizer pressure and level.

From the outcomes of the transient analyses, it can be deduced that it is possible to easily control the system in all the cases examined since the maximum excursions of the main thermal–hydraulic quantities characterising the system are below $\pm 5\%$ and the steady-state pulse conditions are recovered after each transition in a few hundred seconds. The trend of the FW MFR (see Fig. 21) shows some oscillations in cases 1 and 2 that could probably be limited by successive optimisations of the control system. Nevertheless, the average temperature in the primary circuit of the DIV PFC varies between 130.2 °C and 136.3 °C in the worst case (case 1), exhibiting excursions that are below 3 % of its nominal value. The temperature in the hot leg reaches a peak value of 139 °C in case 1 while in all other cases it does not exceed 136 °C.

On the other hand, it is not possible to detect significant pressure variations at the head of the pressurizer given the operating conditions of strongly subcooled fluid associated with extremely modest temperature variations and the variations in the liquid level inside the pressurizer are less than $\pm 5\%$ of the nominal value.

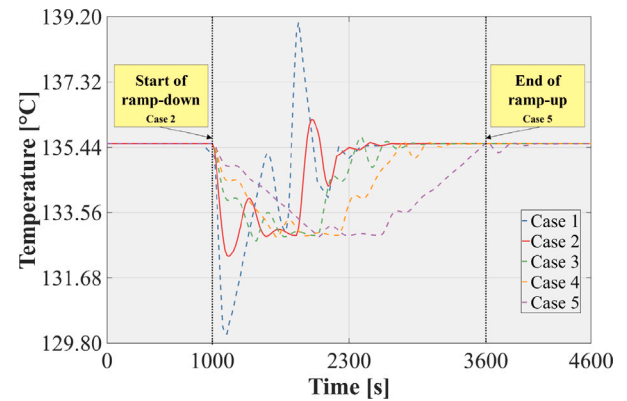


Fig. 20. Hot leg temperature.

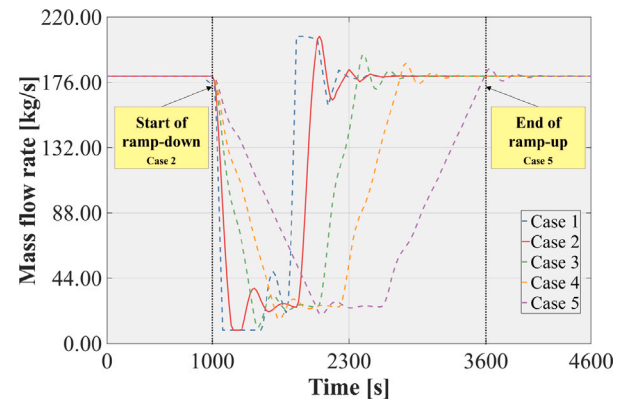


Fig. 21. Feed water mass flow rate.

7. Conclusions and follow-up

Among the activities supported by the EUROfusion consortium, UNIPA, in collaboration with the DCT, has commenced a research campaign to study the thermal–hydraulic performance of the DIV PFC PHTS under normal and upset conditions.

The study has been performed in accordance with a theoretical–computational approach based on the use of the TRACE thermal–hydraulic system code version 5.0 patch 7.

To this end, a detailed finite-volume model has been developed to catch all the relevant geometric, hydraulic and thermal features of components inside and outside the vessel.

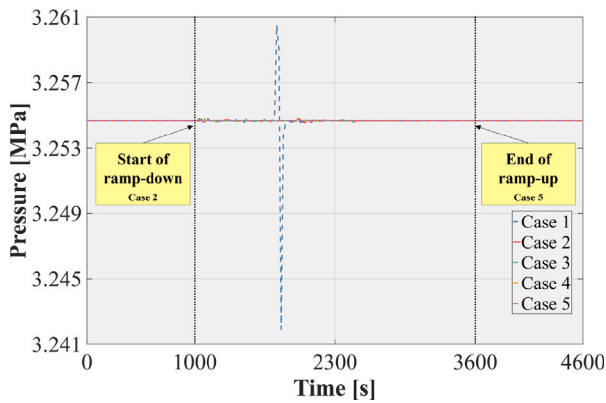


Fig. 22. Pressurizer pressure.

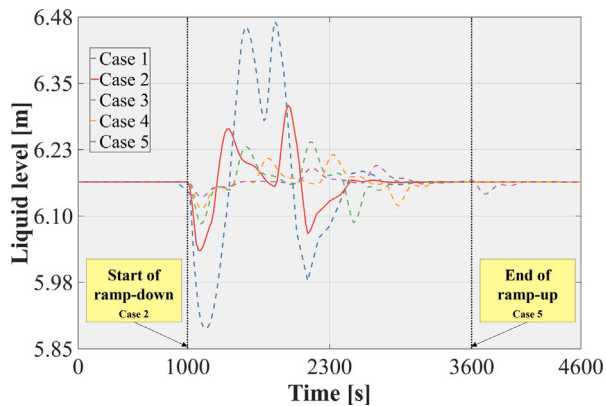


Fig. 23. Pressurizer level.

Afterwards, the study has been concentrated on the analysis of the thermal–hydraulic performance of the DIV PFC PHTS under hypothetical steady-state conditions that are similar to what would be encountered in the pulse phase of the EU-DEMO duty cycle. This part of the activity has provided the opportunity to verify the distribution of MFR among the DIV PFC and the pressure drops along the entire circuit. Furthermore, it has been possible to make a comparison with available analytical data to check the efficaciousness of the created model in forecasting the performance of the DIV PFC PHTS.

In a second phase, efforts have been directed at studying the thermal–hydraulic performances of the DIV PFC PHTS under the transient conditions expected during normal operations and, in particular, a parametric study has been conducted, to evaluate how the duration of the transition phases envisaged during the EU-DEMO duty cycle would affect the relevant thermal–hydraulic features of the system. The results have shown that it is possible to easily control the system in all the cases examined since the maximum excursions of the relevant thermal–hydraulic quantities characterising the system are below $\pm 5\%$ and the steady-state pulse conditions are recovered after each transition in a few hundred seconds.

In spite of this important milestone, it must be pointed out that the design of the divertor in a tokamak is also dependent on several issues other than thermal–hydraulics, therefore studies are ongoing in an attempt to converge towards a divertor design solution able to meet all criteria and requirements imposed by both engineering and plasma physics. Nevertheless, the scientific activity herewith described has demonstrated the ability of the set-up TRACE model to catch the main thermal–hydraulic phenomena characterizing the DIV PFC coolant system during its routine operations.

Future activities are planned to assess the system behaviour during relevant upset and accidental conditions.

CRedit authorship contribution statement

S. Vacca: Writing – original draft, Methodology, Investigation, Conceptualization. **G. Agnello:** Writing – original draft, Methodology, Investigation, Conceptualization. **G. Bongiovì:** Writing – original draft, Methodology, Investigation, Conceptualization. **F.M. Castrovinci:** Writing – original draft, Methodology, Investigation, Conceptualization. **P. Chiovaro:** Writing – original draft, Methodology, Investigation, Conceptualization. **P.A. Di Maio:** Writing – original draft, Methodology, Investigation, Conceptualization. **F. Maviglia:** Writing – original draft, Methodology, Investigation, Conceptualization. **I. Moscato:** Writing – original draft, Methodology, Investigation, Conceptualization. **A. Quartararo:** Writing – original draft, Methodology, Investigation, Conceptualization. **M. Siccinio:** Writing – original draft, Methodology, Investigation, Conceptualization. **E. Vallone:** Writing – original draft, Methodology, Investigation, Conceptualization.

Declaration of competing interest

The authors declare that they have no known competing financial interests or personal relationships that could have appeared to influence the work reported in this paper.

Data availability

Data will be made available on request.

Acknowledgements

This work has been carried out within the framework of the EUROfusion Consortium, funded by the European Union via the Euratom Research and Training Programme (Grant Agreement No 101052200 — EUROfusion). Views and opinions expressed are however those of the author(s) only and do not necessarily reflect those of the European Union or the European Commission. Neither the European Union nor the European Commission can be held responsible for them.

References

- [1] G. Federici, et al., Overview of the DEMO staged design approach in Europe, Nucl. Fusion 59 (2019) 066013, <http://dx.doi.org/10.1088/1741-4326/ab1178>.
- [2] T. Donné, W. Morris, European Research Roadmap to the Realisation of Fusion Energy, ISBN: 978-3-00-061152-0, 2018.
- [3] I. Moscato, et al., Tokamak cooling systems and power conversion system options, Fusion Eng. Des. 178 (2022) 113093, <http://dx.doi.org/10.1016/j.fusengdes.2022.113093>.
- [4] F. Maviglia, et al., Integrated design strategy for EU-DEMO first wall protection from plasma transients, Fusion Eng. Des. 177 (2022) 113067, <http://dx.doi.org/10.1016/j.fusengdes.2022.113067>.
- [5] US Nuclear Regulatory Commission, Trace V5.0 Theory Manual, 2010.
- [6] H. Zohm, et al., The EU strategy for solving the DEMO exhaust problem, Fusion Eng. Des. 166 (2021) 112307, <http://dx.doi.org/10.1016/j.fusengdes.2021.112307>.
- [7] G. Mazzone, et al., Eurofusion-DEMO divertor - Cassette design and integration, Fusion Eng. Des. 157 (2020) 111656, <http://dx.doi.org/10.1016/j.fusengdes.2020.111656>.
- [8] M. Merola, et al., Overview and status of ITER internal components, Fusion Eng. Des. 89 (7) (2014) 890–895, <http://dx.doi.org/10.1016/j.fusengdes.2014.01.055>.
- [9] P. Di Maio, et al., Hydraulic assessment of an upgraded pipework arrangement for the DEMO divertor plasma facing components cooling circuit, Fusion Eng. Des. 168 (2021) 112368, <http://dx.doi.org/10.1016/j.fusengdes.2021.112368>.
- [10] I. Moscato, Divertor PFC PHTS layout and summary tables, 2022, EUROfusion IDM Ref.: 2Q3PQG.
- [11] F. Maviglia, et al., DEMO Plasma Heat Loads, 2020, EUROfusion IDM Ref.: 2NFPNU.
- [12] R. Villari, et al., WPDIV 2020– D005 Divertor Cassette Neutronics Presentation, 2020, EUROfusion IDM Ref.: 2NCWDK.
- [13] M. Siccinio, et al., DEMO PFC Surface Heat Load Specifications, 2020, EUROfusion IDM Ref.: 2P985Q.
- [14] F. Subba, et al., Prediction of Wall Loads During Steady-State Operation in DEMO, 2020, EUROfusion IDM Ref.: 2NDHBC.

- [15] F. Maviglia, et al., Impact of plasma-wall interaction and exhaust on the EU-DEMO design, *Nucl. Mater. Energy* 26 (2021) 100897, <http://dx.doi.org/10.1016/j.nme.2020.100897>.
- [16] G. Preverzev, et al., ASTRA - An Automatic System for Transport Analysis in a Tokamak, 1991, IPP Report 5/42.
- [17] M. Carr, A. Meakins, A. Baciero, C. Giroud, *CHERAB's Documentation*, 2018, Available: <https://cherab.github.io/documentation/index.html>.
- [18] R. Schneider, et al., Plasma edge physics with B2-eirene, *Contrib. Plasma Phys.* 46 (1-2) (2006) 3-191, <http://dx.doi.org/10.1002/ctpp.200610001>.
- [19] T. Berry, et al., Calculation of Decay Heat in PbLi for Entire WCLL Reactor, 2020, EUROfusion IDM Ref.: 2NQL5P.
- [20] I. The MathWorks, *MATLAB Primer*, 2021, Release: R2021b.
- [21] S. D'Amico, et al., Preliminary thermal-hydraulic analysis of the EU-DEMO Helium-Cooled Pebble Bed fusion reactor by using the RELAP5-3D system code, *Fusion Eng. Des.* 162 (2021) 112111, <http://dx.doi.org/10.1016/j.fusengdes.2020.112111>.
- [22] ANSYS Inc, *ANSYS CFX-Solver Theory Guide*, 2020, Release: 2020 R2.
- [23] I.E. Idelchik, *Handbook of Hydraulic Resistance*, Jaico Publishing House, 2008.
- [24] E. Vallone, et al., Development of a thermal-hydraulic model of the EU-DEMO Water Cooled Lithium Lead Breeding Blanket Primary Heat Transport System, *Fusion Eng. Des.* 193 (2023) 113686, <http://dx.doi.org/10.1016/j.fusengdes.2023.113686>.
- [25] V. Gnielinski, New equations flow regime heat and mass transfer in turbulent pipe and channel flow, *Int. J. Chem. Eng.* 16 (1976) 359-368.
- [26] R.M. Manglik, A.E. Bergles, Swirl flow heat transfer and pressure drop with twisted-tape inserts, in: *Advances in Heat Transfer*, vol. 36, Elsevier, 2003, pp. 183-266, [http://dx.doi.org/10.1016/S0065-2717\(02\)80007-7](http://dx.doi.org/10.1016/S0065-2717(02)80007-7).
- [27] D. Groeneveld, et al., The 2006 CHF look-up table, *Nucl. Eng. Des.* 237 (15) (2007) 1909-1922, <http://dx.doi.org/10.1016/j.nucengdes.2007.02.014>.
- [28] T.D. Marshall, D.L. Youchison, L.C. Cadwallader, Modeling the nukiya curve for water-cooled fusion divertor channels, *Fusion Technol.* 39 (2P2) (2001) 849-855, <http://dx.doi.org/10.13182/FST01-A11963345>.
- [29] A. Raffray, et al., Critical heat flux analysis and R&D for the design of the ITER divertor, *Fusion Eng. Des.* 45 (4) (1999) 377-407, [http://dx.doi.org/10.1016/S0920-3796\(99\)00053-8](http://dx.doi.org/10.1016/S0920-3796(99)00053-8).
- [30] F. Castrovinci, et al., Thermal-hydraulic study of the primary heat transport system of the DEMO divertor Cassette body, *Fusion Eng. Des.* 192 (2023) 113733, <http://dx.doi.org/10.1016/j.fusengdes.2023.113733>.